THE JOURNAL OF PHYSICAL CHEMISTRY Letters

Letter

pubs.acs.org/JPCL

Interference and Molecular Transport—A Dynamical View: Time-Dependent Analysis of Disubstituted Benzenes

ShuGuang Chen,[†,§] Yu Zhang,[†,§] SiuKong Koo,[†] Heng Tian,[†] ChiYung Yam,[†] GuanHua Chen,*[,†] and Mark A. Ratner*[,‡]

[†]Department of Chemistry, The University of Hong Kong, Pokfulam Road, Hong Kong, People's Republic of China

[‡]Department of Chemistry, Northwestern University, Evanston Illinois 60208, United States

Supporting Information

ABSTRACT: The primary issue in molecular electronics is measuring and understanding how electrons travel through a single molecule strung between two electrodes. A key area involves electronic interference that occurs when electrons can follow more than one pathway through the molecular entity. When the phases developed along parallel pathways are inequivalent, interference effects can substantially reduce overall conductance. This fundamentally interesting issue can be understood using classical rules of physical organic chemistry, and the subject has been examined broadly. However, there has been little *dynamical* study of such interference effects. Here, we use the simplest electronic structure model to examine the coherent time-dependent transport through meta- and para-linked benzene circuits, and the effects of decoherence. We find that the phase-caused coherence/decoherence behavior is established very quickly (femtoseconds), that the localized dephasing at any site reduces the destructive interference of the meta-linked species (raising the conductance), and that thermal effects are essentially ineffectual for removing coherence effects.

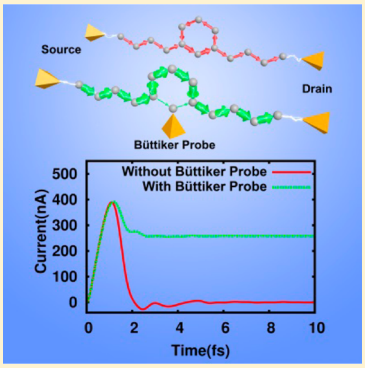

SECTION: Kinetics and Dynamics

Interference behavior in molecular circuits has been examined extensively.[1−34] While simple molecular chains such as alkane or alkene bridges can be understood directly as single pathways, when a ring component is included, multiple charge motion pathways become apparent, and differences in conduction can be observed, depending on how the covalent binding sites on the rings are selected (Figure 1). It has been shown clearly both computationally and experimentally that the conductance can vary substantially for differing binding geometries.[17−29] Analysis of this issue ranges from using concepts of physical organic chemistry to sophisticated approaches based on phase generation.

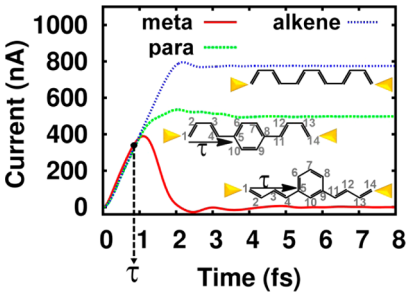

Figure 1. Time-dependent currents through the left electrodes of the meta, para, and alkene systems. The device region contains 14 carbon atoms for meta- or para-, and 12 carbon atoms for the single chain alkene. The bias voltage $\Delta(t)$ is a linear drop across the device region, and is turned on instantaneously in all calculations (i.e., $\Delta(t < 0) = 0$, and $\Delta(t \geq 0) = 0.01$ V). τ is the time when current versus time curves of the three systems diverge, and is the time for an electron to travel from site 1 to site 5 at the Fermi velocity.

We use the quantum Liouville equation to calculate a time-dependent density matrix in the electronic manifold.[35−40] We will use the tight binding (TB) scheme, because it is simple to understand, focuses directly on the interesting π electrons, and gives a clear representation of the coherence, interference, and decoherence behaviors that characterize molecular transport in such structures.

Modeling molecular transport usually uses the Landauer-NEGF computational method.[1−16] The work is nearly always done in the energy representation,[8,41−52] so that the transmission is determined in frequency space and the current follows from the Landauer-NEGF scheme as

$$I = \frac{2e}{h}\int_{-\infty}^{+\infty} Tr\{G^{r}(E, V)\Gamma_{R}G^{a}(E, V)\Gamma_{L}\}\,[f(E - \mu_{R}(V)) - f(E - \mu_{L}(V))]\,dE \quad (1)$$

Here I, V, E, μ, L, and R are respectively the current, the voltage, the relevant energy, the Fermi energy, left, and right. $\Gamma_{L/R}$ represents the spectral density at the left/right linkages

Received: April 9, 2014
Accepted: June 3, 2014
Published: June 3, 2014

   dx.doi.org/10.1021/jz5007143 | J. Phys. Chem. Lett. 2014, 5, 2748−2752

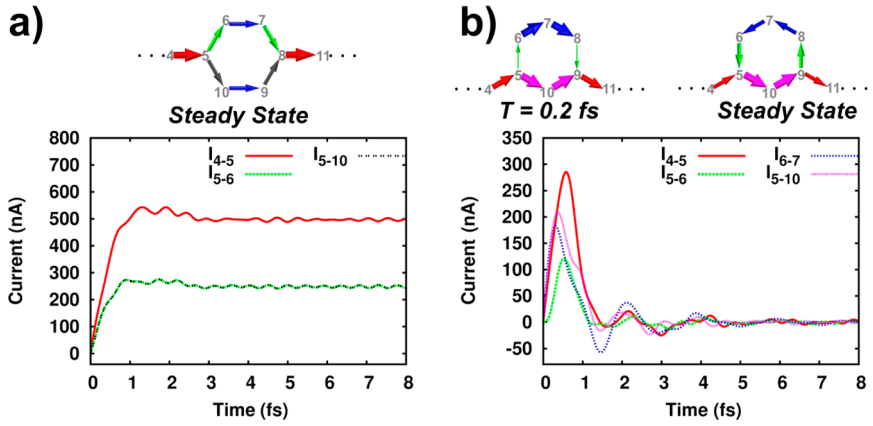

Figure 2. Time-dependent local currents of the para-linkage and meta-linkage systems, and their schematic diagrams in steady state. (a) For para-linkage, all local currents follow the voltage potential. Local currents are exactly the same for the two paths. (b) For meta-linkage, at the beginning, the local currents through both paths follow the voltage potential until the total current I_{4-5} reaches its maximum value ~280 nA. The current then becomes smaller until it reaches the steady state, where the current of the longer path (5−6−7−8−9) reverses direction.

and $G^{r/a}$ is the retarded/advanced Green's function for transport.

In contrast to the energy approach of eq 1, we utilize a time-dependent representation. This is based on solving the following equation of motion for the density matrix (or Liouville equation):[35−40]

$$i\hbar\frac{\mathrm{d}}{\mathrm{d}t}\sigma_{\mathrm{D}}(t) = [h_{\mathrm{D}}(t), \sigma_{\mathrm{D}}(t)] - i\sum_{\alpha=\mathrm{L,R}} Q_{\alpha} \quad (2)$$

where σ_{D} and h_{D} are the reduced density matrix and Fock matrix of the device (D), respectively; Q_{α} is the dissipation term due to the α electrode. Details are given in the Supporting Information. The important interpretation advantage is that these equations give a direct representation of the density at any time. We examine such densities to glean a dynamical understanding of interference.

When vibrational interaction is introduced via polaron-type (Holstein)[53,54] couplings, either at individual carbon atoms or along a given C−C bond, interference effects remain, up to extremely high temperatures. This robustness of coherence in molecules differs substantially from the situation in semiconductor or metallic structures, essentially because the large spacing between molecular energy levels cannot be easily made resonant with vibrational frequencies.

We model electrodes with the simplest spectral density (i.e., wide-band-limit approximation with the coupling strength to the device set to be 2 eV) to mimic the varying strengths of the molecule/electrode couplings. We characterize the electrons using a basis set of one π orbital on each carbon (as in Hückel or Hubbard or PPP models).[55,56] The hopping elements in the TB Hamiltonian are set to be 2 eV. Geometries are based on known structures, and we ignore vibrations, as their effects are expected to be small on interference as the intervals among the molecular energy levels are much larger than the thermal energy. This permits simple closure of the Liouville equation in real time.[36] We start with no net charge on the molecule. The voltage (0.01 V) is then applied as a linear drop from the cathode to the anode, and is turned on instantaneously in all calculations (i.e., $V(t < 0) = 0$, and $V(t \geq 0) = 0.01$ V). The density matrix of the π system is followed as a function of time. In the very short time regime (a few femtoseconds), current growth seems nearly the same for different pathway patterns. Interference manifests itself in a rapid turnover for destructive interference, and a leveling out for constructive interference. When a Büttiker probe (BP)[57] is used to introduce complete decoherence at a given site, the interference patterns disappear, and the dominant pathway provides all the conductance. We observe backflow patterns for destructive interference structures.

Figure 1 shows the behavior of a molecular strand with linear chains of carbons either alone or enclosing a benzene ring, in the para- or meta-configuration. In all three cases, we see an initial rise in the current and steady state is found rapidly: for the para-benzene case, the two parallel pathways reinforce (constructive interference). Note that initially the currents increase linearly with time in all three cases, as seen in our earlier work.[37] At time τ, the currents for para- and meta-linkages deviate from the linear increasing, while the current for alkene continues to increase linearly with time. τ is exactly the time an electron travels at the Fermi velocity from the benzene ring to the end where the measurement takes place. After τ, the electrons from the ring reach the left end, the constructive and destructive interferences kick in for the para- and meta-linkages, respectively, and thus their currents start to deviate from that of the alkene chain.

More interesting behavior occurs in the meta-linked benzene. Transport in such entities has been addressed broadly,[17−29] utilizing NEGF methodology in frequency space. Measured conductance largely agrees with the simple idea of constructive interference in the para-linkage, or destructive interference in the meta-linkage. Here we see the buildup of steady state current, and notice striking interference pathways in Figure 2, which shows true backflow through the longer meta pathway (sites 5−6−7−8−9). The shorter pathway (through site 10) gives positive current, which breaks in half at the exit site 9, with half the current exiting to the downstream electrode and the other half representing a backflow current half of the incoming flux. The striking surge in the current that occurs in the first two femtoseconds rapidly establishes the steady state with a very small residue current: the dynamics of interference requires a finite time to establish itself. The initial current (measured at the left end) comes from the holes in the left linkage, and these holes behave classically, traveling at the Fermi velocity and constant acceleration due to the uniform electric field applied. As a result, the current increases linearly

dx.doi.org/10.1021/jz5007143 | J. Phys. Chem. Lett. 2014, 5, 2748−2752

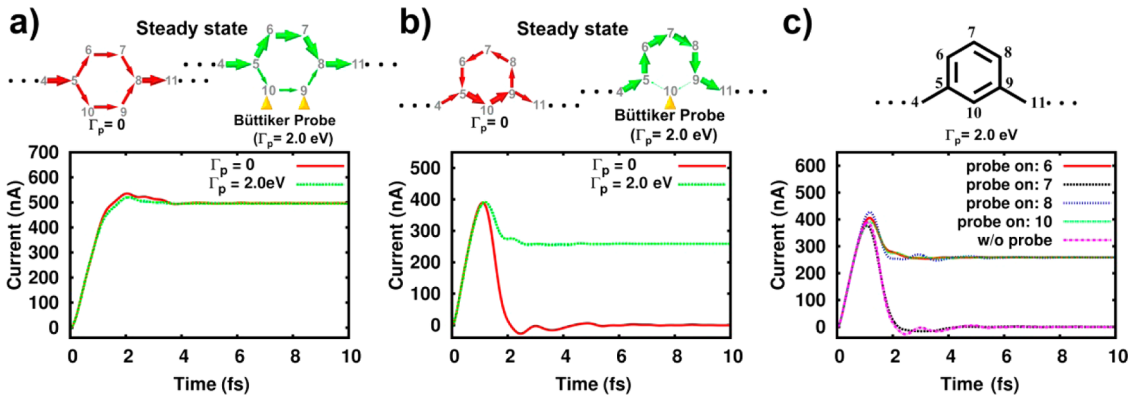

Figure 3. Effects of BP on current. The upper diagrams show the steady-state local current with or without BP, the Figures below show the time-dependent current through the electrodes. (a) For para benzene, the BP is attached to both carbon 9 and carbon 10, to guarantee no net current flowing through the probe due to structural symmetry. (b) BP is attached to carbon 10. (c) BP is attached to different positions of the meta-linked ring with Γ_p = 2.0 eV.

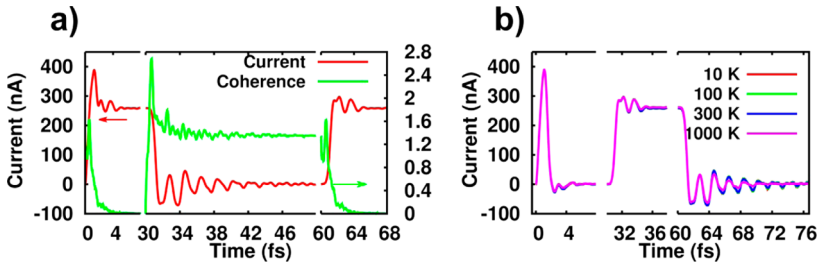

Figure 4. (a) Effects of BP on current and total coherence of the meta-linked benzene system. BP is attached to carbon 10 of the meta-linkage benzene with Γ_p = 2.0 eV. The total coherence is defined as the sum of off-diagonal elements of density matrix. (b) Effects of electron temperature. It is turned off at the initial time and turned on at t = 30 fs. At t = 60 fs, it is turned off again. Temperature is defined by the Fermi–Dirac distribution for the electrodes.

with time until those holes that have been subjected to the destructive interference arrive at the probe at the left end.

The overall currents are much smaller for the meta species of Figure 2 compared to the single pathway (hexatriene), and the equal phase (para) pathways of Figure 1. Phase analyses of the para-, meta-linkage problem have been presented,[28,29] and indeed the phases differ by π, thus providing a negative contribution to the overall response (that is essentially zero in this simulation, but when done in an all-electron calculation corresponds to roughly one percent of the measured current in the para molecule—largely due to σ electrons, which are outside the current model).

Decoherence can occur in real systems by dynamical interaction with a bath, by vibronic behavior (electron/vibration coupling), by inhomogeneities in the environment either static or dynamic, by electronic interaction, and by other molecular substitutions.

To understand the nature of the coherent transport, it is convenient to introduce decoherence, and to observe how the current changes. A useful way to introduce decoherence was put forward by Büttiker,[57] and consists (in the computation) of bringing up a BP structure that destroys the off-diagonal elements of the density matrix at a particular site or sites. It should be mentioned that unlike the direct electron/vibration coupling approach, which does not necessarily produce decoherence,[58,59] the Büttiker probe can guarantee that the phase coherence between the electrons incoming and outcoming is completely destroyed. In this work, we set the magnitude of the line-width function of the BP, Γ_p = 2.0 eV, which is comparable to that of the left or right lead. Figure 3b shows the effects of one BP's on the interferences in the meta-linkage. We see that decoherence can remove the patterns of phase that result in the destructive interference and the strong meta effect, and simply reflect the sum of two pathways that do not conduct so well as two equivalent pathways (para) or one pathway (hexatriene), but obviate the full π-type destructive interference, and conduct substantially better than the decoherence-free meta- linked system.

Figure 3 shows transport through the para-linkage, through the meta-linkage with no dephasing, and with BP dephasing at different sites. The current in the meta-structure increases with BP, and is equal to about 260 nA as shown in Figure 3b (compare with the 490 nA for the para-linkage, Figure 3a). Thus, the BP, by reducing destructive interference, produces a relatively high current. Figure 3c shows what happens when there is one BP, in different sites. Dephasing in this meta-linked system at any of the sites (with the exception of site 7) allows substantial transport through decoherence-based removal of the destructive interference. BP on site 7 has essentially no effect, which indicates that 7 is a decoherence-free site. We calculated the dissipative term for the BP at site 7 in the equation of motion, $Q_{BP}(t) = \varphi_{BP}(t) - \varphi_{BP}^{\dagger}(t)$,[36] and found that it is zero, i.e., $Q_{BP}(t) = 0$. This confirms that the BP at site 7 is indeed decoherence-free. Physically, the current at the site 7 is zero, as the phase of the electronic wave function along the path 5–6–7 differs by π from that along 5–10–9–8–7, just like what occurs at the site 5 or 9. As no current goes through it, the BP at site 7 becomes decoherence-free.

We also examine the dynamics of the electron density with the BP on site 10 of the meta-linkage benzene. At the initial

dx.doi.org/10.1021/jz5007143 | J. Phys. Chem. Lett. 2014, 5, 2748–2752

time, the density rapidly builds up on site 6 and drops on site 8, and slightly later it builds up on site 5 and drops on site 9. Then by symmetry, the populations on sites 10 and 7 should not be affected by the field, and they are not. In comparison, we check the meta-linkage benzene system without the BP, and note that the density dynamics in two cases are similar, despite the fact the current and its dynamics are distinctively different in the presence or absence of the BP (cf. Figure 3b).

Figure 4a shows the dynamics when BP is added and removed, and the correlation between the current and electronic coherence. Here we define the electronic coherence as the sum of the off-diagonal elements of the density matrix, in the representation based on the eigenvectors of the steady state density matrix. For the meta, the current and the electronic coherence take about 6 fs to reach steady values. When the BP is removed (at 30 fs), the current drops (as it should for the meta), and the coherence reaches a value of 1.34. However, both the current and the coherence take about 12 fs to reach their steady state values. When the BP is reinstated, we see coherences oscillate before reaching a steady-state value of zero, and the current also becomes steady, at ∼260 nA, with a time of 6 fs.

Finally, the temperature dependence is of interest, because of possible dephasing. Here we consider an electron temperature—we keep bond lengths and angles constant (a next study will examine the electron/vibron interactions); we examine the meta-linked structure with the BP at site 10. Figure 4b shows very little effect of the hot electrons, even up to T = 1000 K (a clearly unphysical value). Some weak oscillations occur at low temperatures—these are most visible above 60 fs, where the sudden turnoff of the BP causes small oscillations, whose amplitude drops off with increasing T. Eventually, these oscillations dampen out.

In conclusion: the dynamical picture shows that interferences require time to develop: at the beginning, electrons seek their pathways independently, and only interfere with one another once the electrons that have been subjected to the interference arrive at the electric probe. In simple models, destructive interference is strong, and reduces overall transport in the meta to nearly zero. In real systems at room temperature, these effects are seen and are robust (despite thermal motion and interelectronic interaction). For structures involving two rings, measured meta and para transport differed by factors of roughly $10^{2.60}$. The dynamical picture presented here allows understanding how these patterns are developed, and might suggest schemes for which switching could be attained, and strong dynamic control accomplished. The correlation between the magnitude of current and the electronic coherence reveals the quantum interference nature of such electronic structures, and the mechanism of switching. Remaining issues include why these interference effects are so robust, observation at room temperature in solvents, and measurements ranging from molecular transport to intramolecular electron transfer, and should be explored further.

■ ASSOCIATED CONTENT

Ⓢ Supporting Information

Methodology for time-dependent simulations. This material is available free of charge via the Internet at http://pubs.acs.org.

■ AUTHOR INFORMATION

Corresponding Authors

*E-mail: ghc@everest.hku.hk.

*E-mail: ratner@northwestern.edu.

Author Contributions

[§]Authors who contributed equally.

Notes

The authors declare no competing financial interest.

■ ACKNOWLEDGMENTS

We thank the Hong Kong Research Grant Council for support (HKU 700912P, HKU 700711P, HKUST9/CRF/11G, AoE/P-04/08), and M.R. thanks the NSF for support (CHE 1058896). We thank A. Nitzan, V. Mujica, G. Solomon, M. Galperin, T. Hansen, R. Goldstein, D. Andrews, M. Reuter, L. Venkataraman, N. J. Tao, A. Roitberg, Y. Kwok, and R. Wang for helpful discussions and assistance.

■ REFERENCES

(1) Cuevas, J. C.; Scheer, E. *Molecular Electronics: An Introduction to Theory and Experiment*; World Scientific Publishing Company: Singapore, 2010.

(2) Cuniberti, G.; Fagas, G.; Richter, K. Introducing Molecular Electronics: A Brief Overview. *Lect. Notes Phys.* **2005**, *680*, 1.

(3) Datta, S. *Electronic Transport in Mesoscopic Systems*; Cambridge University Press: Cambridge, U.K., 1997.

(4) Datta, S. *Quantum Transport: Atom to Transistor*; Cambridge University Press: Cambridge, U.K., 2005.

(5) Datta, S. *Lessons from Nanoelectronics: A New Perspective on Transport*; World Scientific Publishing Company, Incorporated: Singapore, 2012.

(6) Di Ventra, M. *Electrical Transport in Nanoscale Systems*; Cambridge University Press: Cambridge, U.K., 2008.

(7) Joachim, C.; Gimzewski, J. K.; Aviram, A. Electronics Using Hybrid-Molecular and Mono-Molecular Devices. *Nature* **2000**, *408*, 541−548.

(8) Joachim, C.; Ratner, M. A. Molecular Electronics: Some Views on Transport Junctions and Beyond. *Proc. Natl. Acad. Sci. U.S.A.* **2005**, *102*, 8801−8808.

(9) Li, C.; Mishchenko, A.; Wandlowski, T. Charge Transport in Single Molecular Junctions at the Solid/Liquid Interface. *Top. Curr. Chem.* **2011**, *313*, 121−188.

(10) Liang, G. C.; Ghosh, A. W.; Paulsson, M.; Datta, S. Electrostatic Potential Profiles of Molecular Conductors. *Phys. Rev. B* **2004**, *69*, 115302.

(11) Metzger, R. M. *Unimolecular and Supramolecular Electronics I: Chemistry and Physics Meet at Metal−Molecule Interfaces*; Springer: New York, 2012.

(12) Nitzan, A. *Relaxation, Transfer and Reactions in Condensed Molecular Systems*; OUP Oxford: New York, 2006.

(13) Nitzan, A. Electron Transmission through Molecules and Molecular Interfaces. *Annu. Rev. Phys. Chem.* **2001**, *52*, 681−750.

(14) Ratner, M. A Brief History of Molecular Electronics. *Nat. Nanotechnol.* **2013**, *8*, 378−381.

(15) Reed, M. A.; Zhou, C.; Muller, C. J.; Burgin, T. P.; Tour, J. M. Conductance of a Molecular Junction. *Science* **1997**, *278*, 252−254.

(16) Xue, Y.; Datta, S.; Ratner, M. First-Principles Based Matrix Green's Function Approach to Molecular Electronic Devices: General Formalism. *Chem. Phys.* **2002**, *281*, 151−170.

(17) Vazquez, H.; Skouta, R.; Schneebeli, S.; Kamenetska, M.; Breslow, R.; Venkataraman, L.; Hybertsen, M. S. Probing the Conductance Superposition Law in Single-Molecule Circuits with Parallel Paths. *Nat. Nanotechnol.* **2012**, *7*, 663−667.

(18) Kalyanaraman, C.; Evans, D. G. Molecular Conductance of Dendritic Wires. *Nano Lett.* **2002**, *2*, 437−441.

(19) Sautet, P.; Joachim, C. Electronic Interference Produced by a Benzene Embedded in a Polyacetylene Chain. *Chem. Phys. Lett.* **1988**, *153*, 511−516.

(20) Sautet, P.; Joachim, C. The Sixl-Higelin Salicylideneaniline Molecular Switch Revisited. *Chem. Phys.* **1989**, *135*, 99−108.

(21) Stafford, C. A.; Cardamone, D. M.; Mazumdar, S. The Quantum Interference Effect Transistor. *Nanotechnology* **2007**, *18*, 424014.
(22) Andrews, D. Q.; Solomon, G. C.; Van Duyne, R. P.; Ratner, M. A. Single Molecule Electronics: Increasing Dynamic Range and Switching Speed Using Cross-Conjugated Species. *J. Am. Chem. Soc.* **2008**, *130*, 17309−17319.
(23) Ernzerhof, M.; Zhuang, M.; Rocheleau, P. Side-Chain Effects in Molecular Electronic Devices. *J. Chem. Phys.* **2005**, *123*, 134704.
(24) Guedon, C. M.; Valkenier, H.; Markussen, T.; Thygesen, K. S.; Hummelen, J. C.; van der Molen, S. J. Observation of Quantum Interference in Molecular Charge Transport. *Nat. Nanotechnol.* **2012**, *7*, 305−309.
(25) Markussen, T.; Schiötz, J.; Thygesen, K. S. Electrochemical Control of Quantum Interference in Anthraquinone-Based Molecular Switches. *J. Chem. Phys.* **2010**, *132*, 224104.
(26) Markussen, T.; Stadler, R.; Thygesen, K. S. The Relation between Structure and Quantum Interference in Single Molecule Junctions. *Nano Lett.* **2010**, *10*, 4260−4265.
(27) Cardamone, D. M.; Stafford, C. A.; Mazumdar, S. Controlling Quantum Transport through a Single Molecule. *Nano Lett.* **2006**, *6*, 2422−2426.
(28) Solomon, G. C.; Andrews, D. Q.; Hansen, T.; Goldsmith, R. H.; Wasielewski, M. R.; Van Duyne, R. P.; Ratner, M. A. Understanding Quantum Interference in Coherent Molecular Conduction. *J. Chem. Phys.* **2008**, *129*, 054701.
(29) Solomon, G. C.; Andrews, D. Q.; Van Duyne, R. P.; Ratner, M. A. When Things Are Not as They Seem: Quantum Interference Turns Molecular Electron Transfer "Rules" Upside Down. *J. Am. Chem. Soc.* **2008**, *130*, 7788−7789.
(30) Kocherzhenko, A. A.; Grozema, F. C.; Siebbeles, L. D. A. Charge Transfer through Molecules with Multiple Pathways: Quantum Interference and Dephasing. *J. Phys. Chem. C* **2010**, *114*, 7973−7979.
(31) Zarea, M.; Powell, D.; Renaud, N.; Wasielewski, M. R.; Ratner, M. A. Decoherence and Quantum Interference in a Four-Site Model System: Mechanisms and Turnovers. *J. Phys. Chem. B* **2013**, *117*, 1010−1020.
(32) Kocherzhenko, A. A.; Siebbeles, L. D. A.; Grozema, F. C. Chemically Gated Quantum-Interference-Based Molecular Transistor. *J. Phys. Chem. Lett.* **2011**, *2*, 1753−1756.
(33) Emin, D. Vibrational Dispersion and Small-Polaron Motion: Enhanced Diffusion. *Phys. Rev. B* **1971**, *3*, 1321−1337.
(34) Emin, D. Lattice Relaxation and Small-Polaron Hopping Motion. *Phys. Rev. B* **1971**, *4*, 3639−3651.
(35) Zheng, X.; Wang, F.; Yam, C. Y.; Mo, Y.; Chen, G. Time-Dependent Density-Functional Theory for Open Systems. *Phys. Rev. B* **2007**, *75*, 195127.
(36) Zheng, X.; Chen, G.; Mo, Y.; Koo, S.; Tian, H.; Yam, C.; Yan, Y. Time-Dependent Density Functional Theory for Quantum Transport. *J. Chem. Phys.* **2010**, *133*, 114101−114111.
(37) Chen, S.; Xie, H.; Zhang, Y.; Cui, X.; Chen, G. Quantum Transport through an Array of Quantum Dots. *Nanoscale* **2013**, *5*, 169−173.
(38) Xie, H.; Jiang, F.; Tian, H.; Zheng, X.; Kwok, Y.; Chen, S.; Yam, C.; Yan, Y.; Chen, G. Time-Dependent Quantum Transport: An Efficient Method Based on Liouville−Von-Neumann Equation for Single-Electron Density Matrix. *J. Chem. Phys.* **2012**, *137*, 044113−044110.
(39) Zhang, Y.; Chen, S.; Chen, G. First-Principles Time-Dependent Quantum Transport Theory. *Phys. Rev. B* **2013**, *87*, 085110.
(40) Tian, H.; Chen, G. An Efficient Solution of Liouville−Von Neumann Equation That Is Applicable to Zero and Finite Temperatures. *J. Chem. Phys.* **2012**, *137*, 204114−204116.
(41) Harbola, U.; Esposito, M.; Mukamel, S. Quantum Master Equation for Electron Transport through Quantum Dots and Single Molecules. *Phys. Rev. B* **2006**, *74*, 235309.
(42) Maciejko, J.; Wang, J.; Guo, H. Time-Dependent Quantum Transport Far from Equilibrium: An Exact Nonlinear Response Theory. *Phys. Rev. B* **2006**, *74*, 085324.
(43) Ness, H.; Fisher, A. J. Nonperturbative Evaluation of Stm Tunneling Probabilities from Ab Initio Calculations. *Phys. Rev. B* **1997**, *56*, 12469−12481.
(44) Remacle, F.; Levine, R. D. Electrical Transport in Saturated and Conjugated Molecular Wires. *Faraday Discuss.* **2006**, *131*, 45−67.
(45) Renaud, N.; Ratner, M. A.; Joachim, C. A Time-Dependent Approach to Electronic Transmission in Model Molecular Junctions. *J. Phys. Chem. B* **2011**, *115*, 5582−5592.
(46) Sanchez, C. G.; Stamenova, M.; Sanvito, S.; Bowler, D. R.; Horsfield, A. P.; Todorov, T. Molecular Conduction: Do Time-Dependent Simulations Tell You More Than the Landauer Approach? *J. Chem. Phys.* **2006**, *124*, 214708.
(47) Stratford, K.; Beeby, J. L. A Time-Dependent Approach to Conductance in Narrow Channels. *J. Phys.: Condens. Matter* **1993**, *5*, L289.
(48) Subotnik, J. E.; Hansen, T.; Ratner, M. A.; Nitzan, A. Nonequilibrium Steady State Transport via the Reduced Density Matrix Operator. *J. Chem. Phys.* **2009**, *130*, 144105.
(49) Beratan, D. N.; Skourtis, S. S.; Balabin, I. A.; Balaeff, A.; Keinan, S.; Venkatramani, R.; Xiao, D. Steering Electrons on Moving Pathways. *Acc. Chem. Res.* **2009**, *42*, 1669−1678.
(50) Esposito, M.; Galperin, M. Self-Consistent Quantum Master Equation Approach to Molecular Transport. *J. Phys. Chem. C* **2010**, *114*, 20362−20369.
(51) Monturet, S.; Lorente, N. Inelastic Effects in Electron Transport Studied with Wave Packet Propagation. *Phys. Rev. B* **2008**, *78*, 035445.
(52) Prociuk, A.; Dunietz, B. D. Modeling Time-Dependent Current through Electronic Open Channels Using a Mixed Time-Frequency Solution to the Electronic Equations of Motion. *Phys. Rev. B* **2008**, *78*, 165112.
(53) Emin, D. *Polarons*; Cambridge University Press: Cambridge, U.K., 2012.
(54) Holstein, T. Studies of Polaron Motion: Part I. The Molecular-Crystal Model. *Ann. Phys.* **1959**, *8*, 325−342.
(55) Pariser, R.; Parr, R. G. A Semi-Empirical Theory of the Electronic Spectra and Electronic Structure of Complex Unsaturated Molecules. Ii. *J. Chem. Phys.* **1953**, *21*, 767−776.
(56) Pople, J. A. Electron Interaction in Unsaturated Hydrocarbons. *Trans. Faraday Soc.* **1953**, *49*, 1375−1385.
(57) Büttiker, M. Role of Quantum Coherence in Series Resistors. *Phys. Rev. B* **1986**, *33*, 3020−3026.
(58) Friedman, L.; Holstein, T. Studies of Polaron Motion: Part III: The Hall Mobility of the Small Polaron. *Ann. Phys.* **1963**, *21*, 494−549.
(59) Emin, D. The Hall Mobility of a Small Polaron in a Square Lattice. *Ann. Phys.* **1971**, *64*, 336−395.
(60) Mayor, M.; Weber, H. B.; Reichert, J.; Elbing, M.; von Hänisch, C.; Beckmann, D.; Fischer, M. Electric Current through a Molecular Rod—Relevance of the Position of the Anchor Groups. *Angew. Chem., Int. Ed.* **2003**, *42*, 5834−5838.